CrossMark

Fabrication of reduced graphene oxide/chitosan composite fiber by dry-jet wet spinning

Cuipeng Zhang[1] · Yan Zhang[2] · Xiangyang Hao[1] · Hong Liu[3] · Xiao Lv[1] · Jianfeng Zhu[1] · Wenli Han[1] · Yihe Zhang[1]

Abstract

Reduced graphene oxide (rGO) which was nontoxic, reduced from graphene oxide (GO), and decorated was mixed with chitosan (CS) solution to prepare rGO/chitosan (rGO/CS) biocomposite fiber by dry-jet wet spinning. rGO-/genipin-cross-linked CS (rGO/GCS) composite fiber was prepared. The conditions on nontoxic reduction of GO, namely decoration, spinning, drawing, and nontoxic cross-linking, were studied and optimized. The way to disperse rGO homogeneously in spinning solution was discussed. After surface decorating, rGO was covered by CS without reunion. No phase separation in rGO/CS spinning solution was observed. The solution remained stable for a week after being diluted. The decoration of CS was an effective way to achieve homogeneous dispersion of rGO in solution for spinning. Raman spectroscopy, Fourier-transform infrared spectroscopy (FTIR), X-ray diffraction (XRD), scanning electron microscope (SEM), transmission electron microscopy (TEM), and fluorescence spectroscopy were used to characterize the fibers and their precursors. A series of rGO/CS fibers with a diameter of 0.1 mm were successfully fabricated. The well-dispersed and exfoliated rGO nanosheets were assembled in CS matrix. Both rGO/CS fibers and rGO/GCS fibers maintained the intrinsic fluorescence. Both uncross-linked and cross-linked composite fibers could be bent freely. The work built up the foundation for systematic conductivity and mechanical property research about rGO/CS composite fibers.

Keywords Graphene oxide (GO) · Reduced graphene oxide (rGO) · Chitosan (CS) · rGO-/genipin-cross-linked CS (rGO/GCS) · Composite fiber

1 Introduction

Biodegradable scaffold materials play important roles in nerve transplantation. Scaffold material and seed cells constitute the core of 3D network of tissue engineering. There are certain requirements for scaffold materials, including the following: (1) good biocompatibility, scaffold materials should be nontoxic to cells; (2) good mechanical properties, to meet the needs of operating and supporting cells; (3) controllable biodegradability; and (4) electrical conductivity. Electrical stimulation has been proved to be effective in promoting adhesion, growth, directional differentiation, and the migration of stem cells by clinic studies, which is significantly important to improve remediation. For this purpose, the scaffold material should be electrically conductive. It is extremely challenging for material science and engineering to meet all above requirements [1–6]. Chitosan (CS), a natural macromolecule which is abundant in the chitin shells of shrimp and other crustaceans, is biodegradable, nontoxic, and antibacterial [7–13]. In medicine, it may be useful in bandages to reduce bleeding and as an antibacterial agent; it can also be used to help deliver drugs through the skin. However, the relatively poor mechanical properties and electrical insulation of CS strongly restrict its

✉ Xiangyang Hao
  haoxy@cugb.edu.cn

✉ Yihe Zhang
  zyh@cugb.edu.cn

1 Beijing Key Laboratory of Materials Utilization of Nonmetallic Minerals and Solid Wastes, National Laboratory of Mineral Materials, School of Materials Science and Technology, China University of Geosciences, Beijing 100083, China

2 School of Physical Electronics, University of Electronic Science and Technology of China, Chengdu 610054, China

3 Center of Bio and Micro/Nano Functional Materials, State Key Laboratory of Crystal Materials, Shandong University, Jinan 250013, China

usages as scaffold materials. Here, we propose a strategy to overcome those shortcomings by incorporating graphene (GN) in CS fiber.

GN has extraordinary mechanical and excellent electronic properties and good biocompatibility [14, 15]. Usually, GN is produced by reduction of graphene oxide (GO). Recently, GO has shown great promise for biomedical applications, such as cell imaging and biosensors. With abundant hydrophilic functional groups, such as −COOH and –OH, GO has strong van der Waal interactions with polymers, especially hydrophilic polymers. It is easy to disperse GO in aqueous and some organic solvents. Many studies on GO/CS composites have demonstrated that GO was an efficient nanofiller for reinforcing CS to achieve better mechanical properties without conductivity. Although some GO-reinforced CS materials were claimed to be potentially useful as biomaterials, so far, little work on GN/CS composite has been reported due to its incompatibility and etc. [16–37].

For the reduction of GO to GN, hydrazine, which is toxic, is the most commonly used reducing agent. A nontoxic reduction is important for the application of GN in the field of biomaterials. Here, nontoxic ascorbic acid (LAA) was chosen to be the reducing agent. After reduction, GO lost most –OH and –COOH functional groups, and the formed GN has weak interfacial interaction with polymers. A surface decoration with nontoxic conjugate structure on GN is important to improve its interactions with polymers.

A great deal of reports on electrospun fiber has been published. Electrospun fibers usually have small diameters from a few nanometers to hundreds of nanometers. However, the poor orientation of electrospun fiber makes it difficult to obtain strong fiber for 3D braiding and inconvenient for stem cell to adhere. In comparison, highly drawn fibers of large diameters (from a few micrometers to a few millimeters) could be obtained by dry-jet wet spinning, which promotes the orientation of polymer chains and GN and improves the mechanical and conductive properties of the resulting fiber. Dry-jet wet spun fiber can be woven into a 3D scaffold with controllable patterns and good mechanical performance. The 3D scaffold can be designed and knitted according to damaged nerves, which provides a microenvironment suitable for the orientated growth of stem cells.

Mechanical properties and the degradation speed of CS fibers and its scaffold can be adjusted by cross-linking and braiding structure during post-drawing process [8–13]. Instead of glyoxal, a common cross-linking agent for CS, a nontoxic cross-linking reagent genipin extracted from gardenia fruit was used in this study. So, in this work, we try to make some progress towards preparing biodegradable scaffold fiber for 3D braiding, which is

nontoxic, electrically conductive, and available for mass production in a cheaper way.

2 Experimental

2.1 Materials

CS (deacetylation rate 85%, viscosity 800~1000 mPa/s) was purchased from Huantai Jinhu Crust Co. Ltd., GO aqueous solution was obtained from Leadernano Tech L. L. C (Jining, China). Genipin was provided by Linchuan Zhixin BioTechnology Co, Ltd (Jiangxi, China). Ascorbic acid (LAA) was purchased from Beijing Chemical Reagent Co, Ltd. Other reagents were bought from Sinopharm Chemical Reagent Co, Ltd (Shanghai, China).

2.2 Experimental methods

Flow chart is shown in Fig. 1. After reduction of GO with LAA, CS and acetic acid (HAc) solutions were added and then ultrasonicated. The pH value was adjusted to 7 for rGO decoration and then ultrasonicated until the solution became homogeneous. CS powder and HAc were mixed with decorated rGO solution and distilled water, then stirred to obtain spinning solutions. After filtering and defoaming, spinning solution was transferred into an extruder. The extruded spinning solution entered a coagulation bath. Then, the nascent fiber was washed by passing through a methanol bath. The as-spun fiber was hot drawn in multiple stages. rGO/CS composite fiber without cross-linking was obtained. The drawn fiber was dipped in the solution of genipin and incubated for cross-linking. The cross-linked fiber was rinsed and dried.

2.2.1 Nontoxic reduction of GO and nontoxic decoration of rGO

During the reduction of GO, the functional groups on GO surface continue to decrease; the hydrophobic increases, leading to agglomerating. How to keep a stable dispersion of rGO is very important to prepare spinning solution.

Ordinary decoration of GN (surface-active agent, grafting functional groups, radiation, etc.) helps to form strong interaction between CS and GN and to improve the strength of the composite fibers. For our purpose, the surface decoration must be nontoxic without significantly damaging conjugate structure of GN. Thus, we used CS itself as surface treatment agent and GN stabilizer.

A mixture of 0.4 g GO (aqueous solution of 5 mg/l) and 3.75 g LAA reacted for 6 h at 60 °C, then LAA was washed off. CS and acetic acid (HAc) solutions were added followed by ultrasonication for 30 min using a pulsed horn sonicator.

Fig. 1 Flow chart
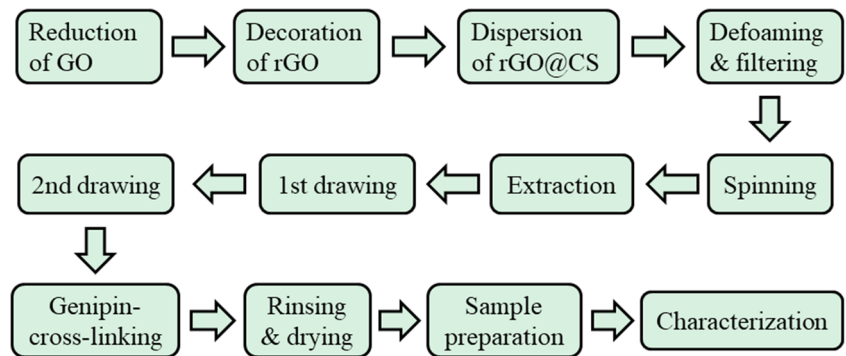
The pH value was adjusted to 7 by NaOH for rGO decoration and then ultrasonicated for 1.5 h until the solution became homogeneous.

3.8% CS powder and 2% HAc, various amounts of decorated rGO solution, and distilled water were mixed together in a flask equipped with an overhead mechanical stirrer and were stirred for 4 h at room temperature to obtain spinning solutions. (All ratios described in the text refer to weight ratio.) By changing the weight fraction of the decorated rGO in CS from 1.1 to 2 to 9% etc., a series of spinning solution, referred as 1.1% rGO/CS, 2% rGO/CS, 9% rGO/CS, etc., was prepared.

2.2.2 Spinning and drawing

After filtering and defoaming, spinning solution was transferred into an extruder. The spinning solution was extruded through an air gap of 3 cm and entered a coagulation bath within a solution of 105 g NaOH, 2 l ethanol (95%), and 1.9 l water. Then, the nascent fiber was washed by passing through a methanol bath at room temperature to remove water. The as-spun fiber was hot drawn in multiple stages by passing through hot water at 60 and at 80 °C, respectively. rGO/CS composite fiber without cross-linking was obtained.

2.2.3 Preparation of genipin-cross-linked rGO/CS composite fiber

The drawn fiber was dipped in the solution of 100 μL genipin (50 mg/ml in ethanol) and incubated for 12 h at 30 °C. The cross-linked fiber was rinsed and dried under vacuum at 40 °C for 48 h.

3 Characterization

FTIR spectra were recorded using an IR spectroscopy (Spectrum 100, PerkinElmer). Raman was carried on LabRAM HR Evolution with an excitation wavelength of 532 nm. The morphologies of the rGO/CS composite fiber were imaged using a SEM (Hitachi S-4800). Samples for cross-sectional view were obtained by tensile fracture in liquid nitrogen. Morphologies of rGO in composite fiber were imaged using a TEM (FEI TECNAI G^2 F30). The structure of the cross-linked and uncross-linked rGO/CS fibers was characterized and compared by using X-ray diffraction (XRD-3, Peking University, 40KV, 16 mA, with a Cu rotating anode parallel focused X-ray source of 1.5418 Å). Fluorescence study was carried out on inverted fluorescence microscopy (LEICA, DMI 6000B). The tensile strength test was on

Fig. 2 Dispersion of rGO in CS solution. **a** CS solution with rGO. **b** CS solution with rGO@CS. **c** CS solution with rGO@CS diluted 1 week later

(a)   (b)   (c)
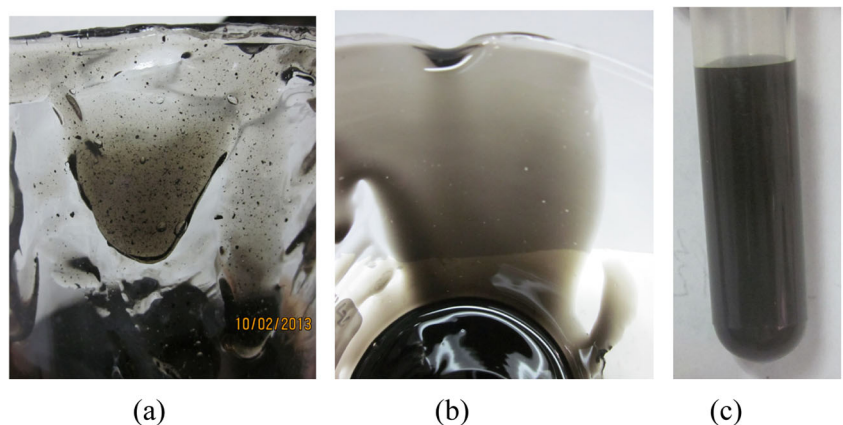
CMT4304, XinSanSi Co. China (which now belongs to MTS Systems Corporation, USA). The electrical resistivity of rGO/CS composite fibers was measured with UT56 Multimeter (UNI-T).

4 Results and discussion

4.1 Nontoxic reduction of GO and nontoxic decoration of rGO

In aqueous solution, along with the reduction of GO, its hydrophobicity increased, leading to agglomeration. In order to keep the stable dispersion of rGO, both the reduction agent and stabilizer agent were simultaneously used during the chemical treatment of rGO.

When rGO was added directly into CS solution, aggregation of rGO appeared, which could be observed by naked eye (Fig. 2a). It is well known that GO with –OH and –COOH groups could be well dispersed in CS. Our initial attempt was to reduce GO in situ in CS matrix by the addition of LAA. But few hours later, the viscosity of rGO/CS blend became too low to draw fiber. It is possible that the LAA lead to the degradation of CS. Thus, we decorated rGO with a small amount of CS right after GO was reduced. After rGO/CS solution washing and sonicating, it was mixed with CS solution. From the wall of the beaker, we can observe that the rGO was dispersed uniformly in the solution (Fig. 2b). The spinning solution is stable after being diluted for 1 week (Fig. 2c). Surface decoration improves the dispersion of rGO in CS solution for spinning.
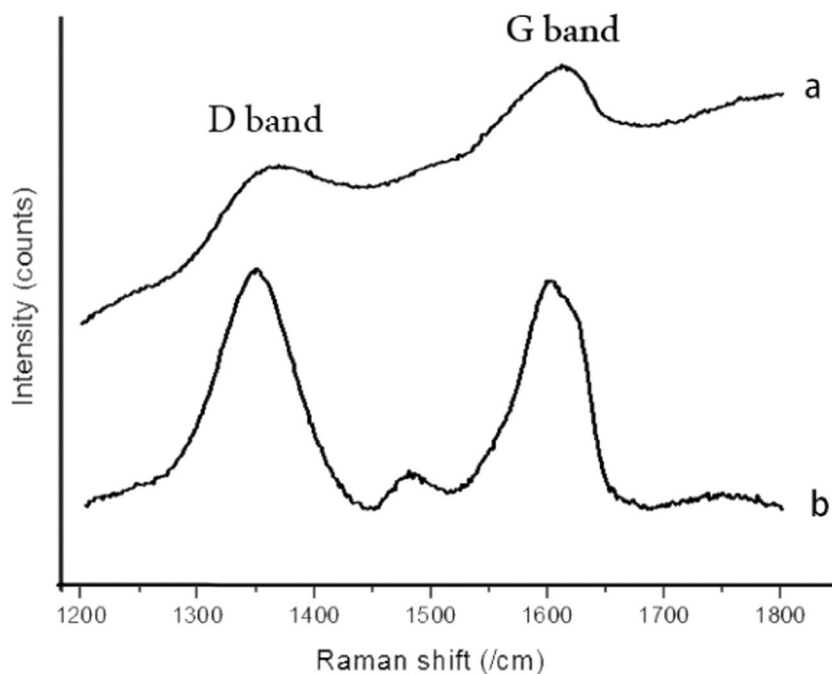
Figure 3 shows the Raman spectra of aqueous solution of GO (a) and aqueous solution of rGO/CS (b). The frequencies of the G band and D band in the rGO/CS are similar to those observed in GO. In panel b, the ratio of D/G achieved dramatic increase compared to that in GO. This change agrees well with Raman spectrum of the GO reduced by hydrazine that was recorded by Stankovich and Guo [17–19], demonstrating that GO was reduced to rGO.

Owing to the strong intrinsic van der Waals forces, nano-sized rGOs always aggregate in most solvents. Even though the rGO/CS blends have been sonicated before surface deposition, rGO still has a strong tendency to form bundles. Chitosan is a linear polysaccharide composed of randomly distributed β-(1→4)-linked D-glucosamine (deacetylated unit) and N-acetyl-D-glucosamine (acetylated unit). Along with the increase of pH, the ionized CS will be deionized and become non-dissolvable in aqueous media. Then, the CS deposits on rGO and forms a CS shell. The interaction between CS and rGO is expected to be strong. Electrostatic attraction among rGO sheets becomes weak after the surface decoration. This is due to the static-repellency of the CS shell. Without the decoration, rGO coagulates even in CS solution.

Combining the properties of rGO and the versatility and biocompatibility of CS, these CS surface-decorated rGO may have broad applications.

4.2 Dry-jet wet spinning and hot drawing

The air gap between spinneret and coagulating bath played an important role for the formation of as-spun fiber. If the dope

Fig. 3 Raman for aqueous solution of GO and rGO@CS. **a** Aqueous solution of GO. **b** Aqueous solution of rGO@CS

Fig. 4 Process condition for fiber. **a** Incomplete solidification of rGO/CS fiber. **b** rGO/CS fiber after the second drawing

(a)　　　　　　　　　　(b)
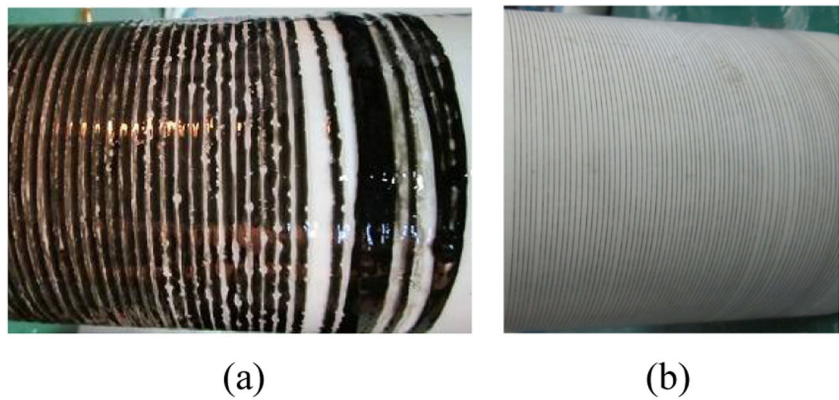
thread was positively drawn (draw ratio > 1), the orientation of chain segments created inside nozzle channel by shear stress would be strengthened in the air gap; as a result, the fiber tenacity would be expected to increase, whereas if the dope thread was negatively drawn (draw ratio < 1), the shear orientation created during nozzle channel would be relaxed in the air gap and then the fiber tenacity would be expected to decrease. The optimal operation parameter values for continuous and stable spinning process are as follows: a spinning speed of 1–3 ml/min, spinneret diameter of 0.86 mm, and reeling velocity of 1–7 m/min.

Both constitution and temperature of coagulating are important factors which affect the fiber tenacity. The very high NaOH concentration or bath temperature made the coagulation of nascent fiber too fast, leading to poor fiber mechanical properties. On the other side, the very low NaOH concentration or bath temperature made the coagulation of the nascent fiber too slow; even the fiber was hardly solidified (Fig. 4a). Hot-drawing process for rGO/CS composite fiber is used to enhance the orientation of CS and rGO.

When temperature of drawing bath increased, the mobility of macromolecules is strengthened and the inner solvent is driven out more easily; thus, the draw ratio and fiber tenacity are increased, but the effect of temperature tends to be leveled off as the temperature reaches above 80 °C. At last, uniform fibers have been obtained (as shown in Fig. 4b).

4.3 Nontoxic cross-linking of rGO/CS composite fiber

Cross-linking is expected to improve the mechanical properties of rGO/CS composite fiber. CS can be cross-linked by bifunctional aldehydes or anhydride. But both reagents are toxic. Genipin, which is extracted from *Eucommia ulmoides*, is nontoxic, can cross-link with CS to form genipin-cross-linked CS (GCS) fiber, and can reduce the antigenicity of implants. Figure 5 shows that the rGO/CS and rGO/GCS composite fiber can be bent freely, indicating that they have good flexibility.

A comparison of infrared spectra between uncross-linked and cross-linked composite fiber is shown in Fig. 6. The dominant peaks at 3405–3360 and 2919–2870 cm^{-1} correspond to stretching vibrations from –OH or –COOH, and –CH_3, respectively. The peaks at 1078–1085 cm^{-1} correspond to C–O–C stretching vibration. The increase in absorbance at 1650–

Fig. 5 Composite fiber can be bent. **a** Uncross-linked 5.3% rGO/CS fiber and **b** cross-linked 5.3% rGO/CS fiber

(a)　　　　　　　　　　(b)

(a)

(b)

(c)
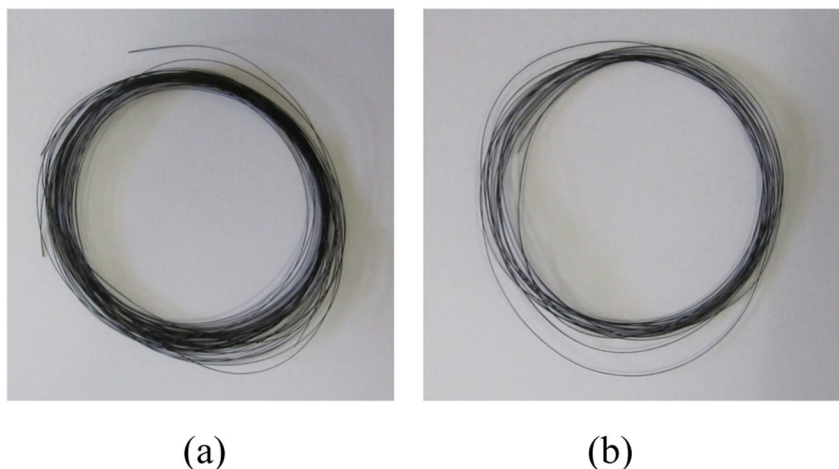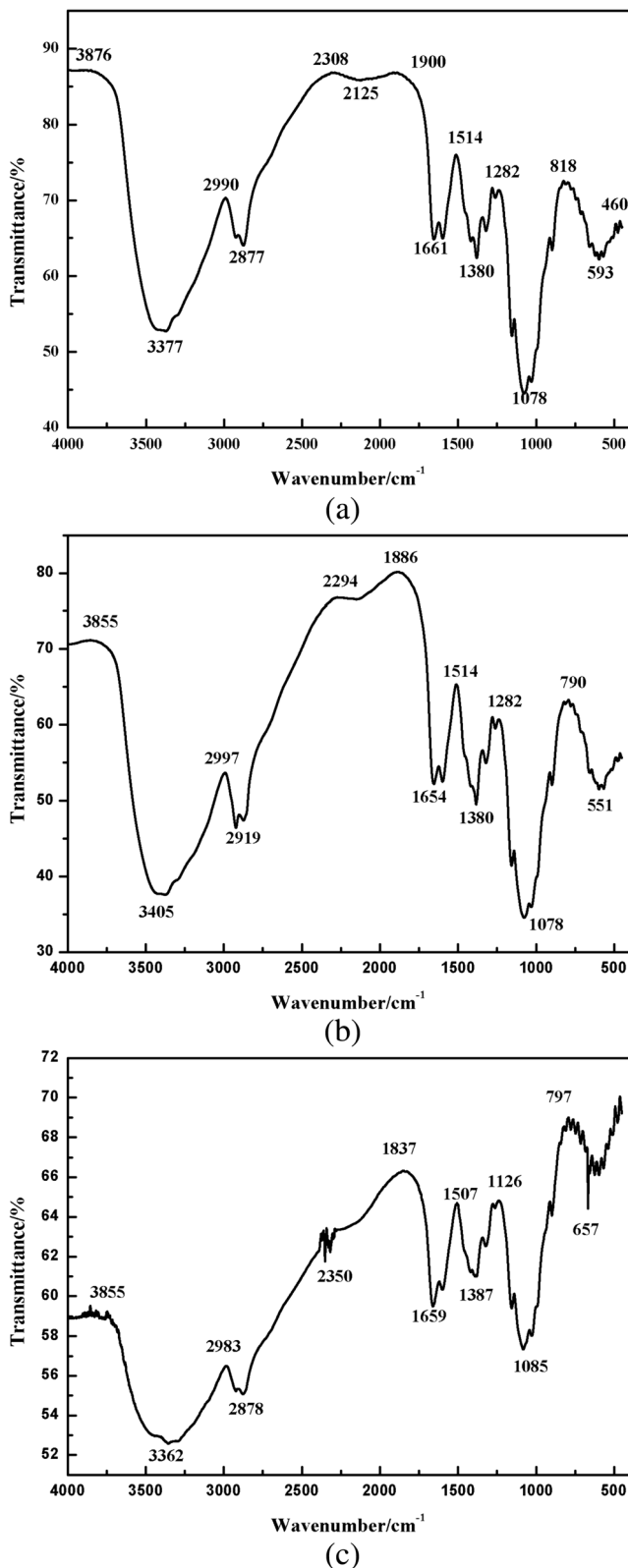
Fig. 6 FTIR of fiber. **a** CS fiber, **b** 1.1% rGO/CS fiber, and **c** 1.1% rGO/GCS fiber
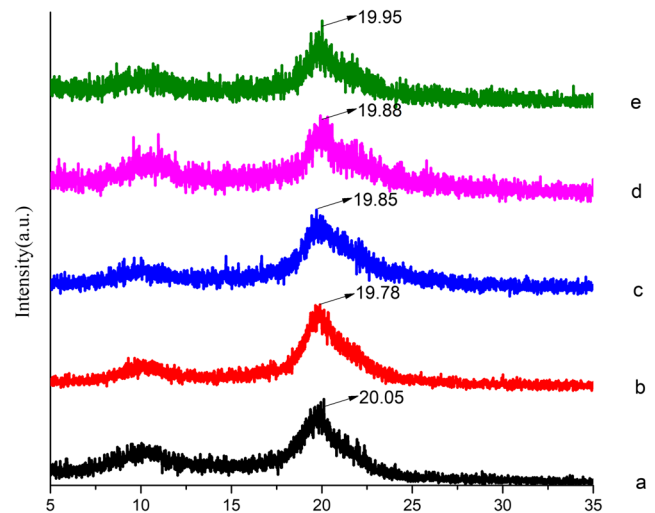

Fig. 7 XRD of fibers. **a** CS fiber, **b** 1.1% rGO/CS fiber, **c** 1.1% rGO/GCS fiber, **d** 9% rGO/CS fiber, and **e** 9% rGO/GCS fiber

1670 cm^{-1} suggests that the amine groups on the CS molecules have been partly converted into the genipin-cross-linked heterocyclic amines.

XRD spectral comparison among CS fiber, 1.1% rGO/CS composite fiber, 1.1% rGO/GCS composite fiber, 9% rGO/CS composite fiber, and 9% rGO/GCS composite fiber is shown in Fig. 7. There are two characteristic diffraction peaks (2θ at about 10 and 20°), which correspond to the type I crystal structure of chitosan (related to the intramolecular hydrogen bonding of chitosan) and the type II crystal structure (related to the intermolecular hydrogen bonding of chitosan), respectively. Focusing on the second peak (2θ at about 20°), we can see, the shift of the second peak is very small. The addition of rGO does not change the crystal structure of chitosan. With the increase of the rGO percentage, the half peak width of the second peak increases to some extent. This indicates the crystallinity of the chitosan in the composite becomes lower than that of the pure chitosan. The addition of excess rGO could lessen the original regularity in chitosan. Cross-linking lowers the regularity as well.

The morphologies of longitudinal section and transverse section of rGO/CS composite fiber are shown in Fig. 8, respectively. SEM photos of composite fiber show the diameter is about 0.1 mm. The cross-section is nearly circular instead of dumbbell shape, the common defect of wet-spinning fiber. The SEM micrographs show that the cross-section of dry-jet wet spun fiber presents a fine texture with little aperture. These results prove that our spinning conditions for preparing rGO/CS composite fiber are optimal. The morphology of uncross-linked fiber is quite coarse, with a lot of grooves on its surface. Longitudinal

Fig. 8 Morphology 1.1% rGO/
CS composite fiber. **a**
Longitudinal section of rGO/CS
fiber. **b** Transverse section of
rGO/CS fiber

(a)   (b)
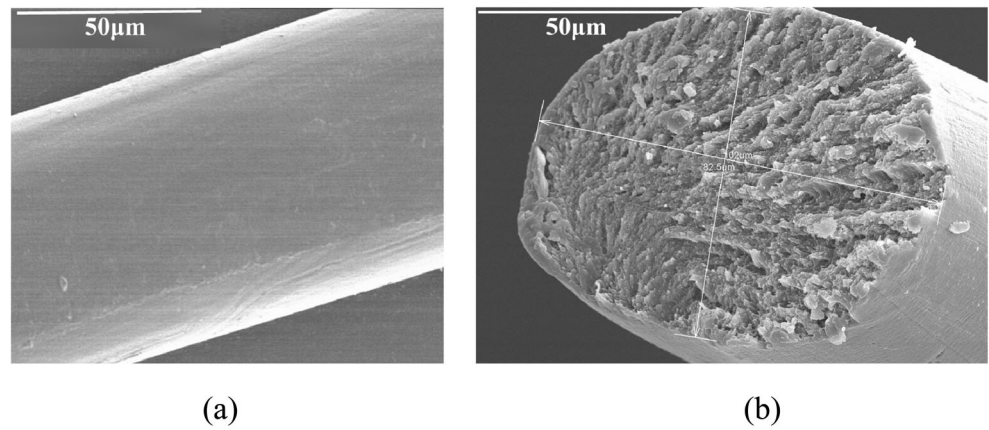
surface of composite fiber is smooth. From TEM photos of composite fiber, rGO can be seen clearly (Fig. 9). The thickness of rGO is several nanometers, and the rGO has exfoliated into nanoscale fillers.

4.4 Fluorescence study

Cross-linked fibers of the rGO/GCS with different rGO loadings have visible fluorescence (Fig. 10). CS-genipin conjugates show a new intrinsic fluorescent property. Genipin is an aglycone derived from an iridoid glycoside. It reacts with the primary amine groups on CS through a nucleophilic attack

to open the dihydropyran ring and forms heterocyclic rings containing nitrogen. It suggests the formation of π–π^* conjugations during decoration reactions, which leads to the fluorescence from the cross-linked CS.

The well-dispersed rGO sheets divide the large conjugated groups into smaller ones. Thus, the fluorescence intensity of the composite fibers decreases along with the increase of rGO loading. On the other hand, rGO sheets quench the intensity of the excitation light. Although fluorescence intensity reduced, rGO-incorporated samples are still highly visible. This fluorescent property of rGO/GCS exhibits advantages for biomedical and bioimaging appli-
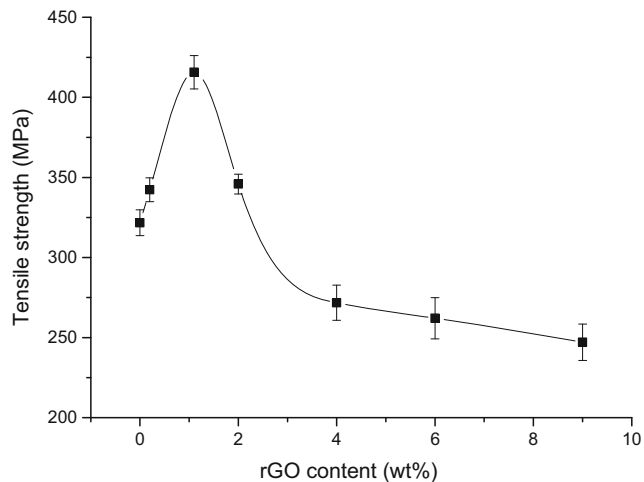
Fig. 9 TEM of rGO/CS composite fiber. **a** Uncross-linked 3% rGO/CS fiber. **b** Cross-linked 3% rGO/CS fiber

(a)   (b)

(a)   (b)   (c)   (d)
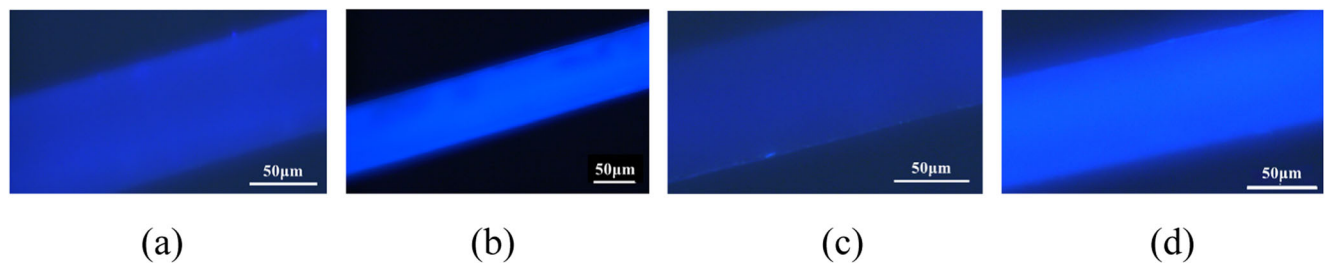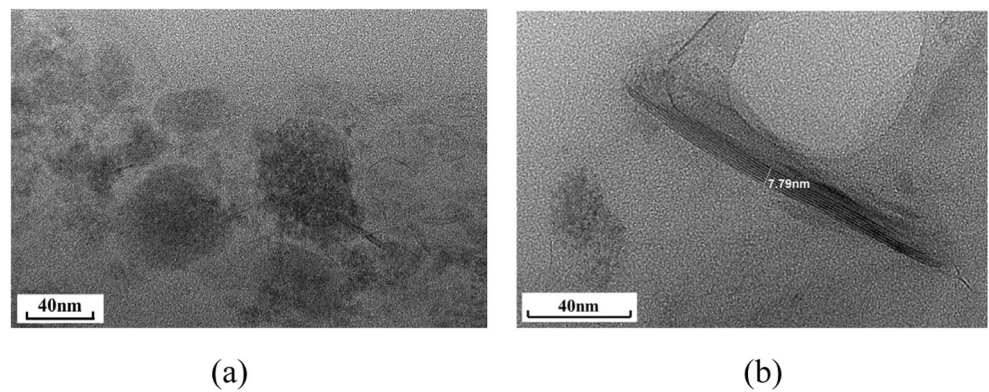
Fig. 10 Fluorescence of rGO/CS composite fiber. **a** Uncross-linked 2% rGO/CS fiber. **b** Cross-linked 2% rGO/CS (2% rGO/GCS) fiber. **c** Uncross-linked 4% rGO/CS fiber. **d** Cross-linked 4% rGO/CS (4% rGO/GCS) fiber

Fig. 11 Tensile strength of rGO/CS composite fiber

cations. Degradation of rGO/GCS scaffold may be investigated outside body in future.

4.5 Mechanical properties and electron conduction

Primary results showed that tensile strength of fibers made by dry-jet wet spinning is much better than that of film [17]. rGO helps enhance the mechanical property of CS fiber (Fig. 11). The electrical resistivity of rGO/CS composite fiber with of 33% rGO is 1809 Ω/cm. rGO/CS with rGO of 29% does not conduct electricity. Systematical research on mechanical properties and conductive properties of composite fiber will be studied later.

5 Conclusions

After surface decorating, rGO is covered by CS without reunion. There is no visible phase separation in rGO/CS spinning solution. The solution is stable after being diluted even after a week. The decoration of CS is an effective way to achieve homogeneous dispersion of rGO in solution for spinning. A series of rGO/CS fibers with a diameter of 0.1 mm has fabricated by a dry-jet wet spinning successfully. A better process condition has been obtained. The well-dispersed and exfoliated rGO nanosheets are assembled in CS matrix. Both rGO/CS fibers and rGO/GCS fibers maintain the intrinsic fluorescence. Both uncross-linked and cross-linked composite fibers can be bent freely. The work lays the foundation for further research on other properties of rGO/CS composite fibers.

Compliance with ethical standards

Conflict of interest The authors declare that they have no conflict of interest.

References

1. Dvir T, Timko B, Kohane D, Langer R (2011) Nanotechnological strategies for engineering complex tissues. Nat Nanotechnol 69:13–22
2. Guilak F, Cohen D, Estes B, Gimble J, Liedtke W, Chen C (2009) Control of stem cell fate by physical interaction with the extracellular matrix. Cell Stem Cell 5:17–26
3. Engler A, Sen S, Sweeney H, Dischr D (2006) Matrix elasticity directs stem cell lineage specification. Cell 126:677–689
4. Moutos F, Freed L, Guilak F (2007) A biomimetic three-dimensional woven composite scaffold for functional tissue engineering of cartilage. Nat Mater 6:162–167
5. Krachenbuehl T, Langer R, Ferreira L (2011) Three-dimensional biomaterials for the study of human pluripotent stem cells. Nat Methods 8:731–736
6. Tuzlakoglu K, Alves C, Mano J, Reis R (2004) Production and characterization of chitosan fibers and 3-D fiber mesh scaffolds for tissue engineering applications. Macromol Biosci 4:811–819
7. Suh J, Matthew H (2000) Application of chitosan-based polysaccharide biomaterials in cartilage tissue engineering: a review. Biomaterials 21:2589–2598
8. Kumar R (2000) A review of chitin and chitosan applications. React Funct Polym 46:1–27
9. Lauto A, Ohebshalom M, Esposito M, Mingin J, Li P, Felsen D, Goldstein M, Poppas D (2001) Self-expandable chitosan stent: design and preparation. Biomaterials 22:1869–1874
10. Tada D, Singh S, Nagesha D, Jost E, Levy C, Gultepe E, Cormack R, Makrigiorgos G, Sridhar S (2010) Chitosan film containing poly (D, L-lactic-co-glycolic acid) nanoparticles: a platform for localized dual-drug release, Pharm Res 27: 1738–1745
11. Jin J, Song M, Hourston D (2004) Novel chitosan-based films cross-linked by genipin with improved physical properties. Biomacromolecules 5:162–168
12. Mi F, Tan Y, Liang H, Sung H (2002) In vivo biocompatibility and degradability of a novel injectable-chitosan-based implant. Biomaterials 23:181–191
13. Wang G, Zheng L, Zhao H, Miao J, Sun C, Ren N, Wang J, Liu H, Tao X (2011) In vitro assessment of the differentiation potential of bone marrow-derived mesenchymal stem cells on genipin-chitosan conjugation scaffold with surface hydroxyapatite nanostructure for bone tissue engineering. Tissue Eng Part A 17:1341–1349
14. Li N, Zhang Q, Gao S, Song Q, Huang R, Wang L, Liu L, Dai J, Tang M, Cheng G (2013) Three-dimensional graphene foam as a biocompatible and conductive scaffold for neural stem cells. Sci Rep 3:1604
15. Chang Y, Yang S, Liu J, Dong E, Wang Y, Cao A, Liu Y, Wang H (2011) In vitro toxicity evaluation of graphene oxide on A549 cells. Toxicol Lett 200:201–210
16. Feng L, Liu Z (2011) Graphene in biomedicine: opportunities and challenges. Nanomedicine 6:317–324
17. Li J, Ren N, Qiu J, Mou X, Liu H (2013) Graphene oxide-reinforced biodegradable genipin-cross-linked chitosan fluorescent biocomposite film and its cytocompatibility. Int J Nanomedicine 8: 3415–3426
18. Geim A, Novoselov K (2007) The rise of graphene. Nat Mater 6: 183–191

19. Stankovich S, Dikin D, Piner R, Kohlhaas K, Kleinhammes A, Kevin A, Jia Y, Wu Y, Nguyen S, Ruoff R (2007) Synthesis of graphene-based nanosheets via chemical reduction of exfoliated graphite oxide. Carbon 45:1558–1565

20. Zhang J, Yang H, Shen G, Cheng P, Zhang J, Guo S (2010) Reduction of graphene oxide via L-ascorbic acid. Chem Commun 46:1112–1114

21. Guo H, Wang X, Qian Q, Wang F, Xia X (2009) A green approach to the synthesis of graphene nanosheets. ACS Nano 3:2653–2659

22. Guo S, Wen D, Zhai Y, Dong S, Wang E (2010) Platinum nanoparticle ensemble-on-graphene hybrid nanosheet: one-pot, rapid synthesis, and used as new electrode material for electrochemical sensing. ACS Nano 4:3959–3968

23. Park S, Ruoff R (2009) Chemical methods for the production of graphenes. Nat Nanotechnol 4:217–224

24. Sun X, Liu Z, Welsher K, Robinson J, Goodwin A, Zaric S, Dai H (2008) Nano-graphene oxide for cellular imaging and drug delivery. Nano Res 1:203–212

25. Zhang L, Xia J, Zhao Q, Liu L, Zhang Z (2010) Functional graphene oxide as a nanocarrier for controlled loading and targeted delivery of mixed anticancer drugs. Small 6:537–544

26. Rana V, Choi M, Kong J, Kim G, Kim M, Kim S (2011) Synthesis and drug-delivery behavior of chitosan-functionalized graphene oxide hybrid nanosheets. Macromol Mater Eng 296:131–140

27. Wang Y, Li Z, Hu D, Lin C, Li J, Lin Y (2010) Aptamer/graphene oxide nanocomplex for in situ molecular probing in living cells. J Am Chem Soc 132:9274–9276

28. Zhang J, Zhang F, Yang H, Huang X, Liu H, Zhang J, Guo S (2010) Graphene oxide as a matrix for enzyme immobilization. Langmuir 26:6083–6085

29. Zhang Y, Zhang J, Huang X, Zhou X, Wu H, Guo S (2012) Assembly of graphene oxide-enzyme conjugates through hydrophobic interaction. Small 8:154–159

30. Wan Y, Wang Y, Wu J, Zhang D (2011) Graphene oxide sheet-mediated silver enhancement for application to electrochemical biosensors. Anal Chem 83:648–653

31. Song W, Li D, Li Y, Li Y, Long Y (2011) Disposable biosensor based on graphene oxide conjugated with tyrosinase assembled gold nanoparticles. Biosens Bioelectron 26:3181–3186

32. Dreyer D, Park S, Bielawski C, Ruoff R (2010) The chemistry of graphene oxide. Chem Soc Rev 39:228–240

33. Xu Y, Hong W, Bai H, Li C, Shi G (2009) Strong and ductile poly (vinyl alcohol)/graphene oxide composite films with a layered structure. Carbon 47:3538–3543

34. Depan D, Girase B, Shah J, Misra R (2011) Structure-process-property relationship of the polar graphene oxide-mediated cellular response and stimulated growth of osteoblasts on hybrid chitosan network structure nanocomposite scaffolds. Acta Biomater 7:3432–3445

35. Deng L, Wang K, Zhao C, Yan H, Britten J, Xu G (2011) Phase and texture of solution-processed copper phthalocyanine thin films investigated by two- dimensional grazing incidence X-ray diffraction. Crystals 1:112–119

36. Zhao C, Xiao S, Xu G (2015) Density of organic thin films in organic photovoltaics. J Appl Phys 118:044510

37. Zhao C, Wang K, Britten J, Zhi M, Wang X, Chen Z, Xu G (2012) Dual nanostructures in poly (3-hexylthiophene) based organic photovoltaics under alternative current electric field. Thin Solid Films 520:5770–5774